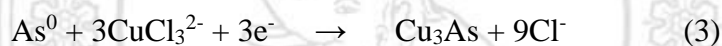# CHAPTER 3

# Results and discussion

## 3. 1 Optimization cathodic stripping voltammetric system for determination of inorganic arsenic in the presence of $Cu^{II}$ and Na-DDTC

The objective of this work was to develop CSV method for determination of inorganic arsenic using a HMDE in the presence of $Cu^{II}$ and Na-DDTC complex. The instrument was setup as described in section 2.4 and the parameters in CSV for arsenic analysis as shown in Table 3.1 were employed.

Table 3.1 Conditions for CSV for determination of arsenic

| Parameter | Conditions |
|---|---|
| Electrode: | |
| Working electrode | Hanging mercury drop electrode |
| Reference electrode | Ag/AgCl |
| Auxiliary electrode | Pt |
| Purging time | 300 s |
| Stirring rate | 2,000 rpm |
| Equilibration time | 10 s |
| Voltage step | 2 mV |
| Amplitude | 20 mV |
| Frequency | 140 Hz |
| Sweep rate | 277.8 mV s$^{-1}$ |
| Waveform | square wave |
| Scanning potential: | |
| Initial potential | - 400 mV |
| End potential | -1000 mV |

The principle of CSV method using HMDE for determination of arsenic is as follow. Arsenic cannot be preconcentrated directly at a mercury electrode because of its low solubility, a preconcentration based on the formation of an intermetallic compound with selenium [38] or copper [44-48] was used. In this work, the copper system was chosen. In the deposition step, $As^{III}$ is electrochemically reduced to $As^0$ while $Cu^{II}$ is reduced to $Cu^0$. The $As^0$ and Cu(Hg) deposited onto Hg electrode, they could form intermetallic compounds with difference Cu:As ratios ($Cu_xAs_y$), depending on the experimental conditions (i.e., concentration of the supporting electrolyte, Cu concentration, deposition potential). The formation of Cu-As intermetallic compounds is shown as follows:

$$H_3AsO_3 + 3H^+ + 3e^- \quad \rightarrow \quad As^0 + 3H_2O \qquad (1)$$

$$Cu^{2+} + Hg + 2e^- \quad \rightarrow \quad Cu(Hg) \qquad (2)$$

$$As^0 + 3CuCl_3^{2-} + 3e^- \quad \rightarrow \quad Cu_3As + 9Cl^- \qquad (3)$$

In the stripping step, the potential is scanned cathodically the $As^0$ is reduced to arsine as follow:

$$Cu_3As + 3H^+ + Hg + 3e^- \quad \rightarrow \quad 3Cu(Hg) + AsH_3 \qquad (4)$$
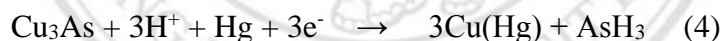
The presence of Na-DDTC in supporting electrolyte causes an increase of $As^{III}$ peak current. Because $As^{III}$ and Na-DDTC could form complex, that is adsorbed at the HMDE in the deposition step and stripped out during the cathodic potential scan undergoing an irreversible reduction [5-6]. A voltammogram recorded during stripping step at peak potential of about -0.82 V (vs. Ag/AgCl) was directly proportional to $As^{III}$ concentration. Some parameters were studied as follow:

23

### 3.1.1 Deposition potential

The arsenic peak current depends on the deposition potential. The effect of deposition potential was studied with 30 µg L$^{-1}$ of As$^{III}$ and the potential was optimized in the range of -0.30 to -0.60 V as shown in Figure 3.1. The peak current decreased at deposition potentials more positive than -0.40 V was probably due to incomplete reduction of As$^{III}$ to As$^0$. At the deposition potentials more negative than -0.40 V, peak current decreased due to the reduction of As$^0$ to arsine during the deposition step. Therefore, a deposition potential of -0.40 V was selected for the next experiment. A deposition time of 60 s was chosen because it was sufficient to obtain the good sensitivity without a considerable increase in the analysis time [47].
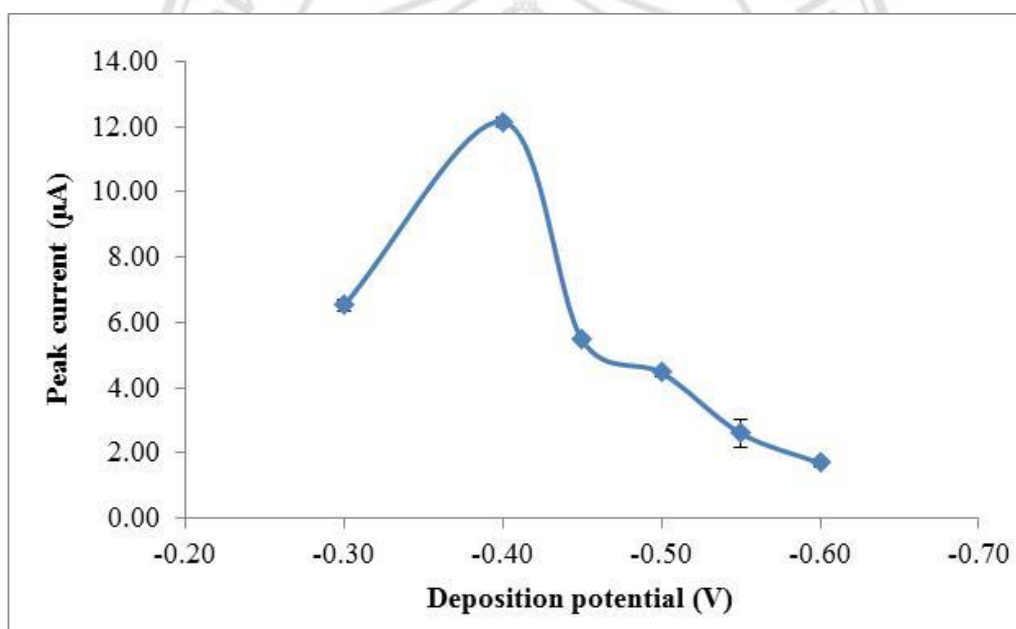


Figure 3.1 Effect of deposition potential on the SWCSV at 30 µg L$^{-1}$ of As$^{III}$ in 1.0 mol L$^{-1}$ HCl, 30 mg L$^{-1}$ Cu$^{II}$; deposition time 60 s

### 3.1.2 Concentration of hydrochloric acid

Hydrochloric acid is used as supporting electrolyte because chloride assists stabilize the $Cu^I$ which needed for formation of the Cu-As intermetallic compounds (equation 3). Effect of hydrochloric acid concentration was studied by varying its concentration in the range of 0.5 to 2.0 mol $L^{-1}$. It was found that although the high HCl concentration gave higher current, it resulted in a more variation in peak current of 20 $\mu g\ L^{-1}\ As^{III}$. The relative standard deviations (%RSD) (n=10) of peak current when using 0.5, 1.0, 1.5 and 2.0 mol $L^{-1}$ HCl were 8.7, 2.4, 10.8 and 10.0%, respectively as shown in Table 3.2. For this reason, a concentration of 1.0 mol $L^{-1}$ HCl was taken as optimum for further studies.

Table 3.2 Effect of hydrochloric acid concentration

| Concentration of hydrochloric acid (mol $L^{-1}$) | Peak current ($\mu A$) | % RSD (n=10) |
|---|---|---|
| 0.5 | 1.93 | 8.7 |
| 1.0 | 4.53 | 2.4 |
| 1.5 | 5.30 | 10.8 |
| 2.0 | 8.43 | 10.0 |

### 3.1.3 Concentration of $Cu^{II}$

The effect of $Cu^{II}$ concentration on the sensitivity of $As^{III}$ determination was investigated, by considering calibration graphs of 5 to 20 µg $L^{-1}$ $As^{III}$ in electrolyte solutions containing 1.0 mol $L^{-1}$ HCl with different concentrations of $Cu^{II}$. A plot of the slope of the calibration graph versus concentration of $Cu^{II}$ is shown in Figure 3.2. It was found that $Cu^{II}$ concentration is a critical parameter affecting the sensitivity of $As^{III}$ determination. An electrolyte solution containing 30 mg $L^{-1}$ $Cu^{II}$ provided the highest sensitivity. This should be due to the in-situ deposition of $Cu^{II}$ on HMDE to form intermetallic compounds with $As^{III}$. However, the higher concentration of $Cu^{II}$ caused a decrease in sensitivity. This might be because of the formation of the intermetallic compounds of higher Cu:As ratio which may not easily to be reduced in the stripping step. Therefore, the concentration of $Cu^{II}$ at 30 mg $L^{-1}$ was chosen to next experiment.
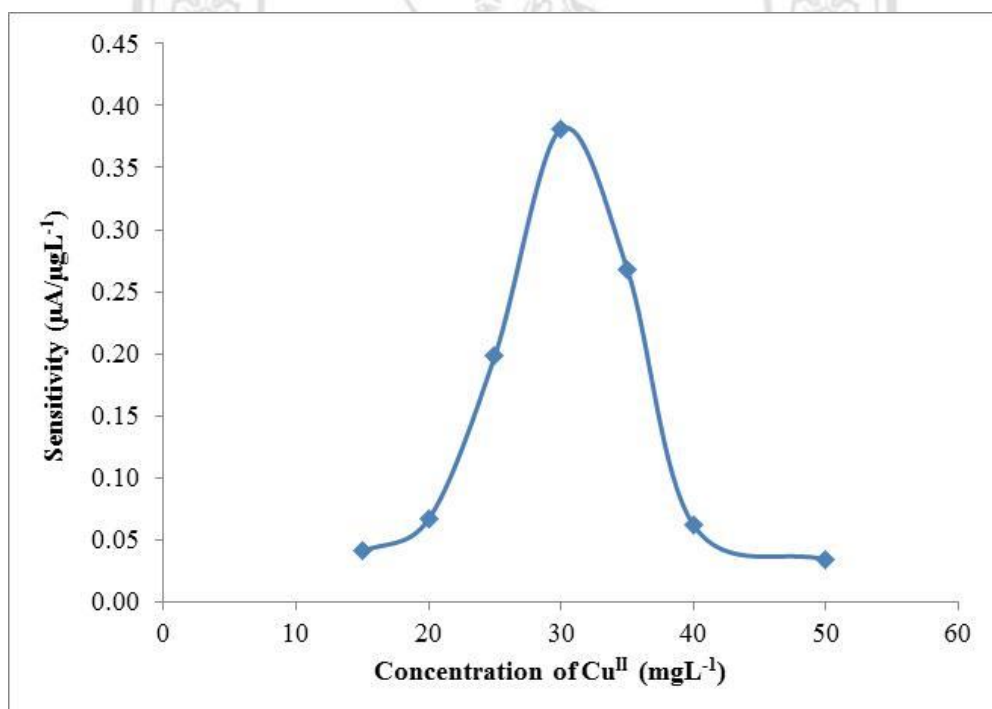


Figure 3.2 Effect of $Cu^{II}$ concentration on the sensitivity of $As^{III}$ determination in 1.0 mol $L^{-1}$ HCl; deposition time 60 s

### 3.1.4 Concentration of thiosulfate

$As^V$ is not electroactive, therefore, the $As^V$ was determined after reduction of $As^V$ to $As^{III}$ in CSV procedure. Several reducing agents are not stable, require high working temperature and interfere in the As determination step. In this work, thiosulfate ($S_2O_3^{2-}$) was used because it is stable, more convenient reductant which allowed fast and complete reduction of $As^V$ to $As^{III}$ at room temperature and without interfering of excess thiosulfate in the subsequent arsenic determination [47]. The effect of thiosulfate concentration was studied for reduction of 30 $\mu g\ L^{-1}$ $As^V$ with reduction time of 300 s. It was found that 10 mg $L^{-1}$ $S_2O_3^{2-}$ concentration as the reducing agent is sufficient for quantitative purpose as shown in Figure 3.3.
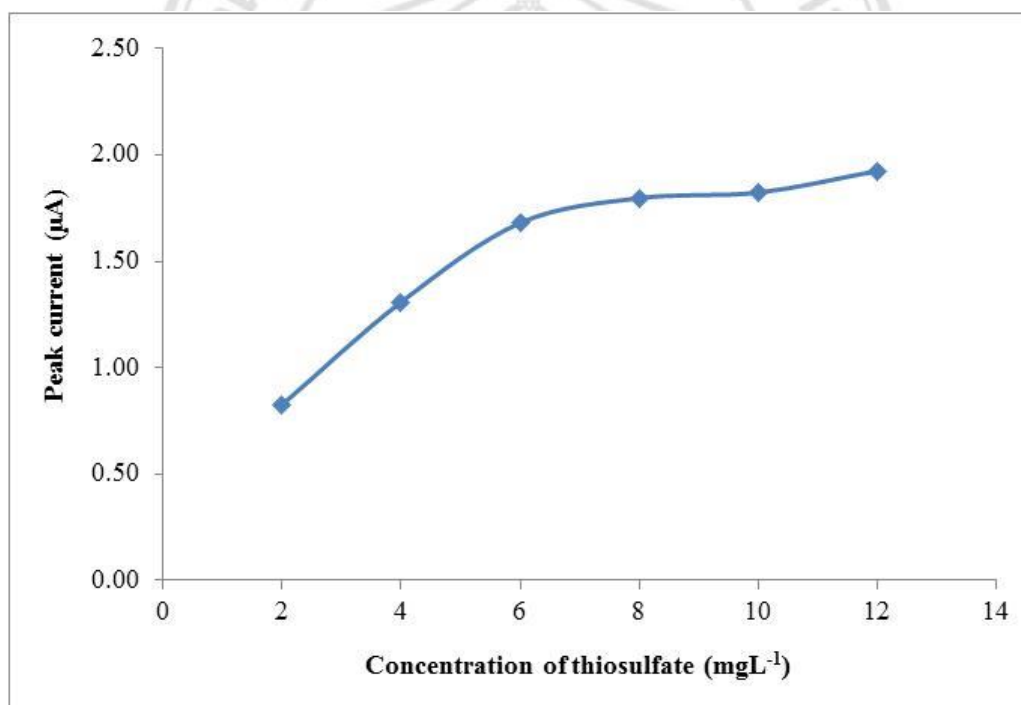


Figure 3.3 Effect of thiosulfate concentration on the SWCSV peak current of 30 $\mu g\ L^{-1}$ $As^V$ in 1.0 mol $L^{-1}$ HCl, 30 mg $L^{-1}$ $Cu^{II}$; reducing time 300 s

### 3.1.5 Reduction time

Reduction time is the time to quantitatively reduced $As^V$ to $As^{III}$, the reduction time was studied in the range of 60 to 420 s with 10 mg $L^{-1}$ $S_2O_3^{2-}$ in electrolyte solutions containing 30 μg $L^{-1}$ $As^V$, 1.0 mol $L^{-1}$ HCl, 30 mg $L^{-1}$ $Cu^{II}$ as shown in Figure 3.4. It was verified that 300 s was sufficient to the quantitative reduction of $As^V$ to $As^{III}$ in the supporting electrolyte.
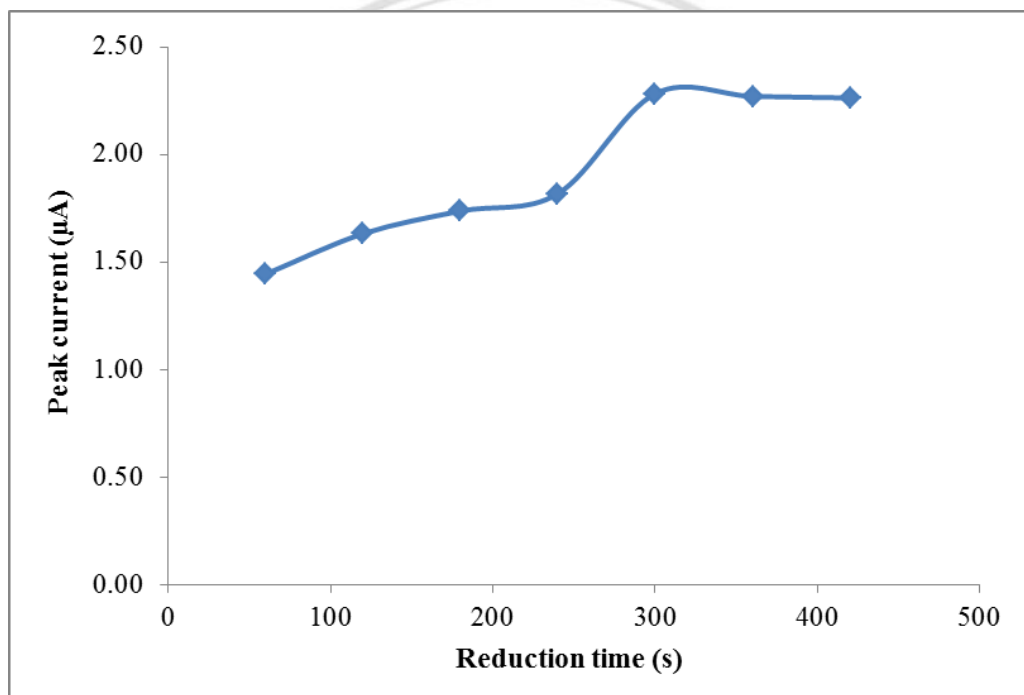


Figure 3.4 Effect of reduction time on the SWCSV peak current of 30 μg $L^{-1}$ $As^V$ in 1.0 mol $L^{-1}$ HCl, 30 mg $L^{-1}$ $Cu^{II}$ and 10 mg $L^{-1}$ $S_2O_3^{2-}$

### 3.1.6 Concentration of Na-DDTC

In the CSV for arsenic determination, Na-DDTC as complexing agent presence in supporting electrolyte caused an increase of peak current of $As^{III}$ and peak potential shifts slightly towards more negative when adding Na-DDTC in the medium. As shown in Figure 3.5, the voltammograms of 20 µg $L^{-1}$ $As^{III}$ in absence of Na-DDTC (a) and presence of 5 µg $L^{-1}$ Na-DDTC (b) were recorded. The effect of Na-DDTC concentration was studied in the range of 1 to 30 µg $L^{-1}$ with 1.0 mol $L^{-1}$ HCl, 30 mg $L^{-1}$ $Cu^{II}$ as shown in Figure 3.6. It was found that the peak currents increased with the increase of Na-DDTC concentration, Na-DDTC could help to improve the formation of complexes with $As^{III}$ in acid medium, that complexes might adsorbed at the HMDE in the deposition period. However, Na-DDTC could form complexes with both copper and arsenic, the mechanism of this system are not quite clear [5]. Thus, the concentration of Na-DDTC at 5 µg $L^{-1}$ was selected.



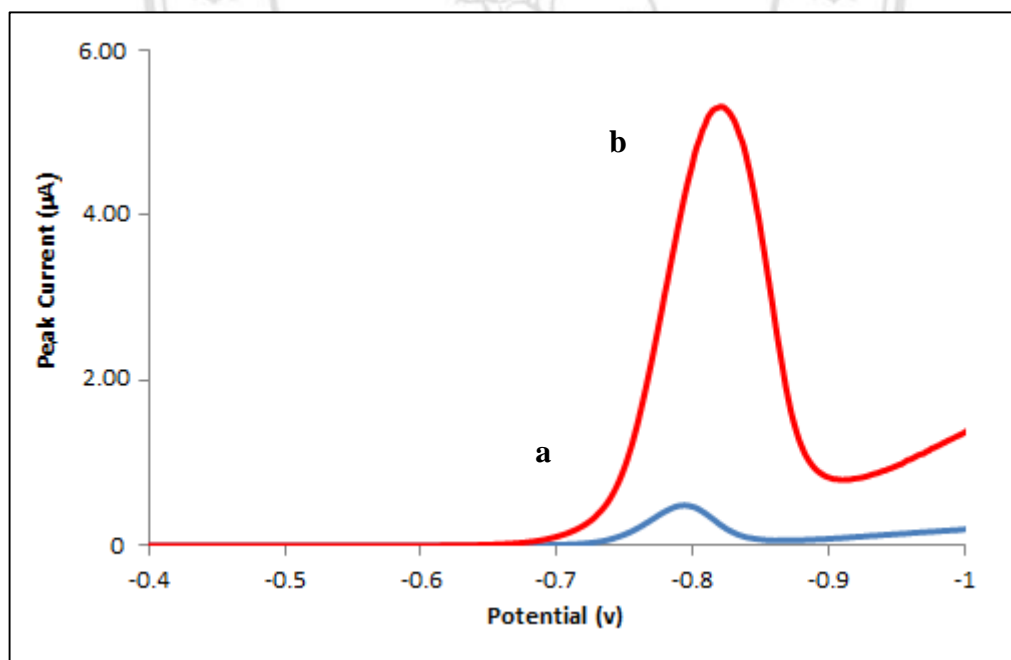Figure 3.5 Voltammogram for concentration Na-DDTC (a) 0; (b) 5 µg $L^{-1}$ in supporting electrolyte: 20 µg $L^{-1}$ of $As^{III}$, 1.0 mol $L^{-1}$ HCl, 30 mg $L^{-1}$ $Cu^{II}$; deposition time 60 s
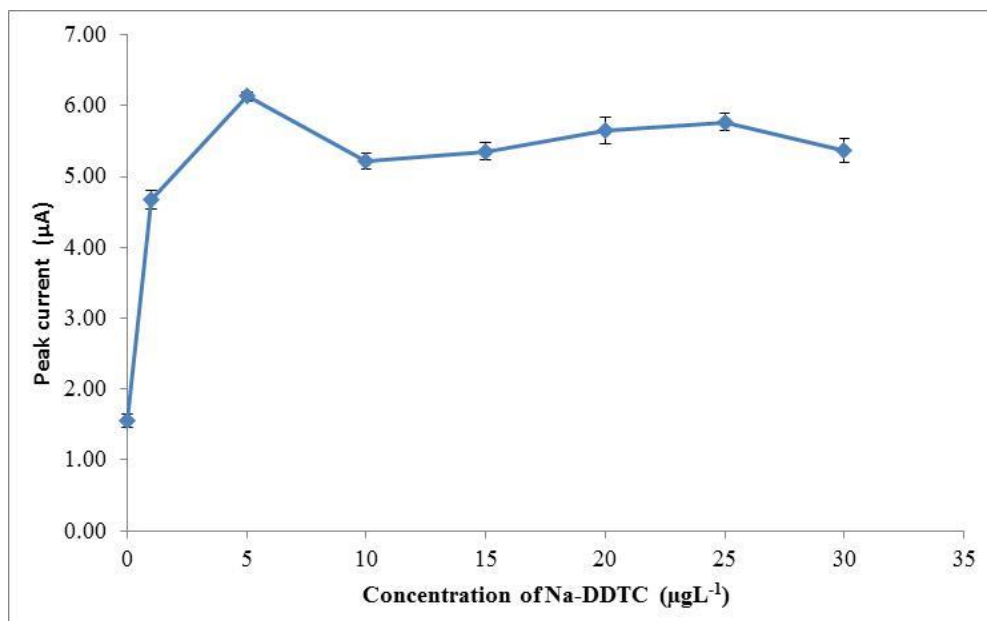
29

Figure 3.6 Effect of Na-DDTC concentration on the SWCSV peak current of 5 μg L⁻¹
As$^{III}$ in 1.0 mol L⁻¹ HCl, 30 mg L⁻¹ Cu$^{II}$; deposition time 60 s

### 3.1.7 The optimum operation conditions

The parameters which affected analytical performance and the optimum condition
for determination of arsenic using CSV with HMDE as a working electrode are
summarized in the Table 3.3.

Table 3.3 Optimization of CSV system using HMDE as a working electrode for
determination of arsenic

| Parameter | Optimum value |
|---|---|
| Deposition potential | -0.40 V |
| Deposition time | 60 s |
| Concentration of hydrochloric acid | 1.0 mol L⁻¹ |
| Concentration of Cu$^{II}$ | 30 mg L⁻¹ |
| Concentration of thiosulfate | 10 mg L⁻¹ |
| Reduction time | 300 s |
| Concentration of DDTC | 5 μg L⁻¹ |

30

### 3.1.8 Analytical characteristics of the system

The CSV system for determination of inorganic arsenic by using HMDE in a supporting electrolyte containing 1.0 mol L$^{-1}$ HCl and 30 mg L$^{-1}$ Cu$^{II}$, voltammograms of As$^{III}$ in concentration range of 2 to 30 μg L$^{-1}$ were recorded as shown in Figure 3.7. A linear calibration graph (y = 0.2921x+0.5014; r$^2$ = 0.9921) was obtained (Figure 3.8).

LOD was calculated from the linear regression of the calibration curve [58]. The LOD of the proposed method was found to be 0.45 μg L$^{-1}$. The results are given in Appendix A.



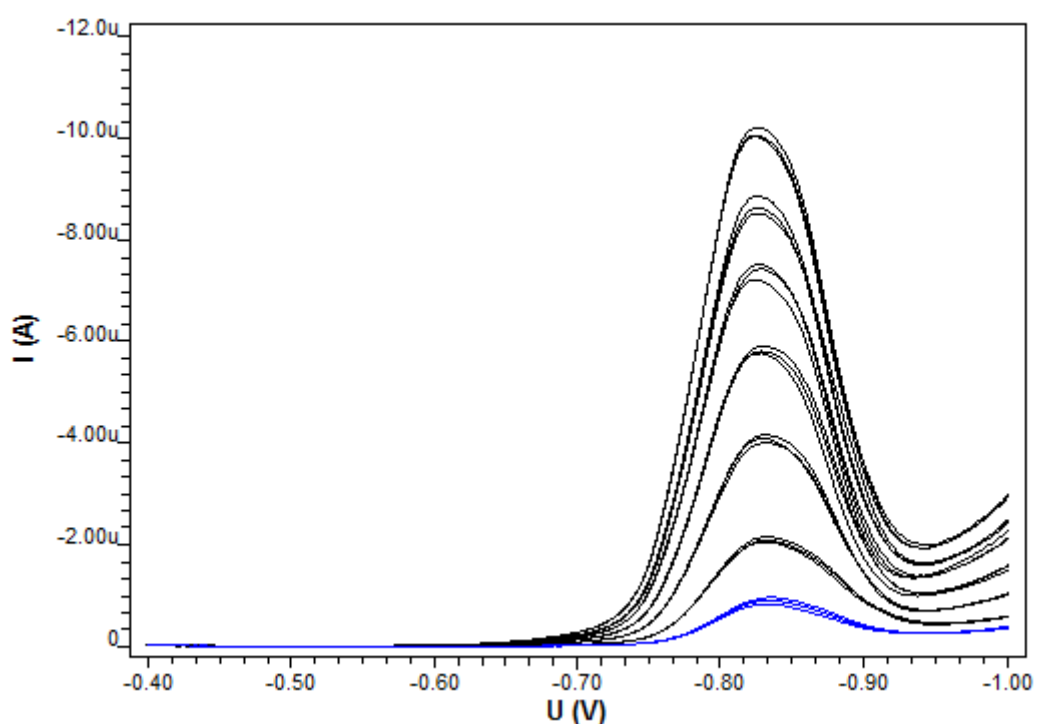Figure 3.7 Voltammograms of As$^{III}$ in concentration range of 2 to 30 μg L$^{-1}$
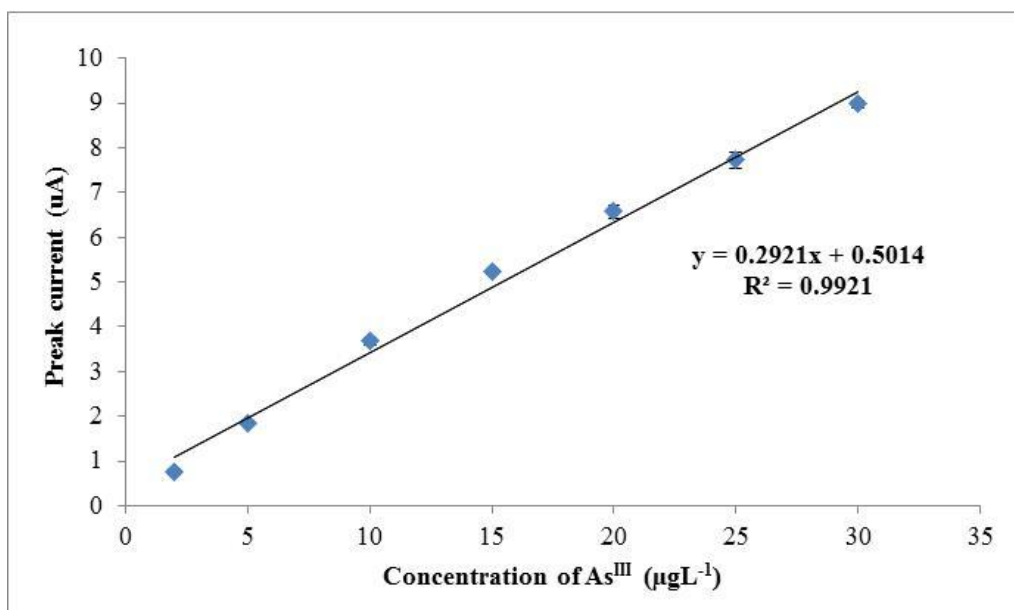
Figure 3.8 Calibration graph of As$^{III}$ determination by SWCSV employing HMDE as a working electrode

The CSV system for determination of As$^{III}$ by using HMDE in a supporting electrolyte containing 1.0 mol L$^{-1}$ HCl, 30 mg L$^{-1}$ Cu$^{II}$ and 5 μg L$^{-1}$ Na-DDTC, voltammograms of As$^{III}$ in concentration range of 0.1 to 0.6 μg L$^{-1}$ were recorded as shown in Figure 3.9. A linear calibration graph (y = 2.7241x + 0.2428; r$^2$ = 0.999) was obtained (Figure 3.10). The LOD was found to be 0.22 ng L$^{-1}$. The results are given in Appendix B.
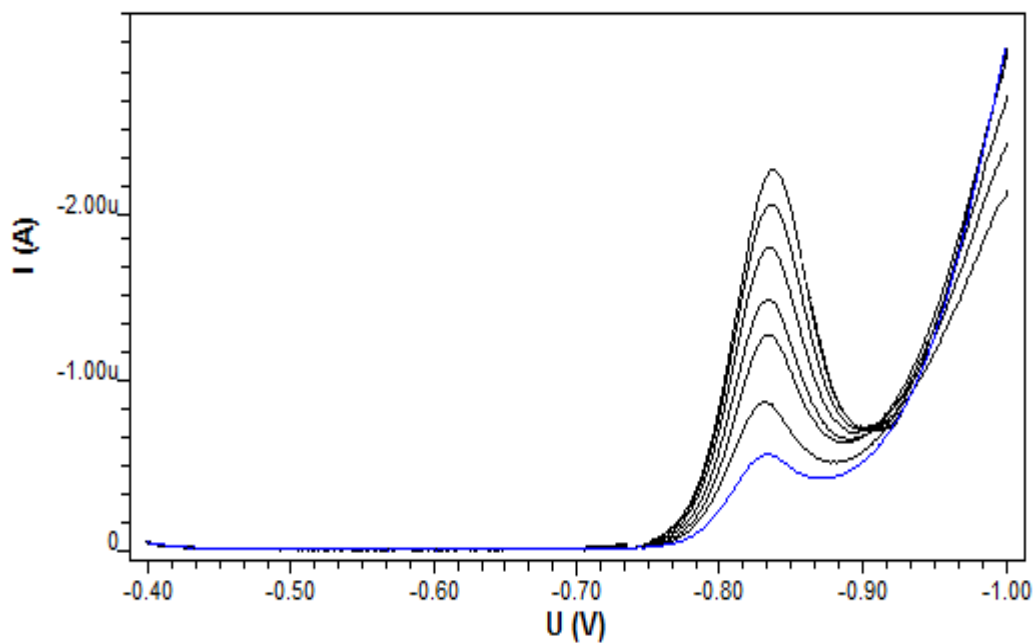
Figure 3.9 Voltammograms of As$^{III}$ in concentration range of 0 to 0.6 µg L$^{-1}$
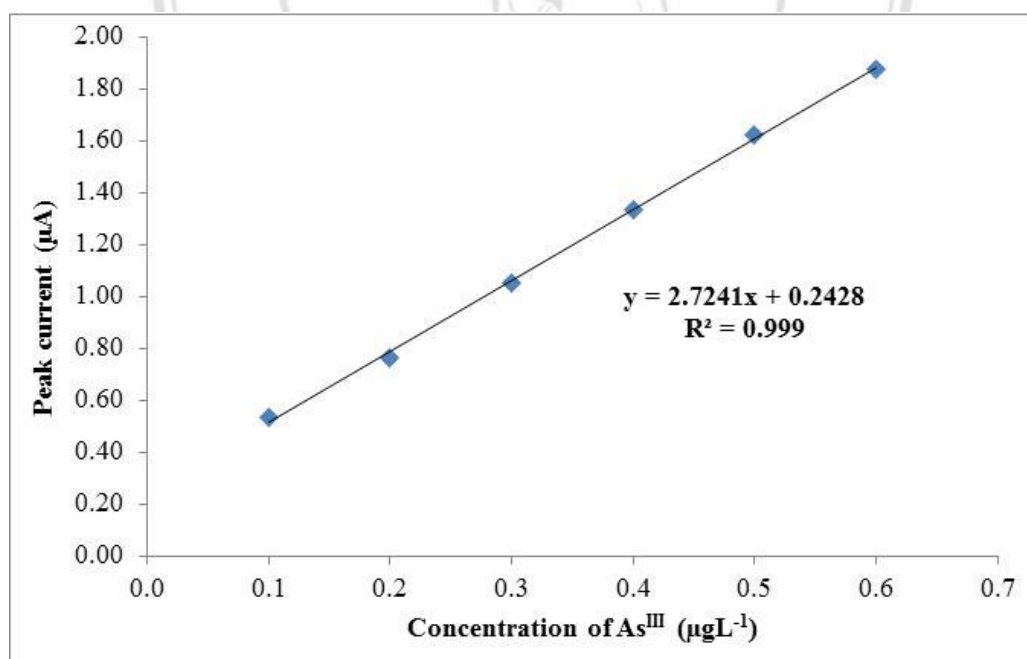


$y = 2.7241x + 0.2428$
$R^2 = 0.999$

Figure 3.10 Calibration graph of As$^{III}$ determination by SWCSV employing HMDE as working electrode containing of 5 µg L$^{-1}$ Na-DDTC in supporting electrolyte

### 3.1.9 An attempt to apply for real sample

After conditions of $As^{III}$ analysis by CSV was optimized, these selected conditions were applied to determine $As^{III}$ in water sample. Unfortunately, it was found that the peak current of $As^{III}$ decrease from μA to nA, might be due to the mercury electrode problem. Several attempts have been made to solve this problem;

a) The efficiency of the HMDE electrode and analytical reproducibility were checked with the determination of Zn by ASV. After that, it was found that the peak current of $As^{III}$ are still very low and not reproducible.

b) The new mercury electrode was used to determine $As^{III}$. However, the peak current of $As^{III}$ are also lower and the presence of noise signal was found. An investigation on the troble of electrode did not help to improve the peak current of $As^{III}$.

Then, the assumption that the low peak current of $As^{III}$ may cause from oxidation of $As^{III}$ to $As^{V}$ was tested. This might be because of the oxidation of $As^{III}$ by chloride in supporting electrolyte [59]. Therefore, the reducing agent was added in solution for reducing $As^{V}$ to $As^{III}$ before analysis of $As^{III}$ because $As^{V}$ is electroinactive species. It was found that the peak current of $As^{III}$ decrease consecutively.

In addition, the unsuitable deposition potential might cause the low peak current. The deposition potential was investigated again. It was found that the deposition potential at -0.35 V, that shifts towards more positive potential from the previous study, provided high peak current of $As^{III}$ but giving poor reproducibility. The alternative way for improve performance of $As^{III}$ determination was studied. The bismuth film electrode (BiFE) was used instead of mercury electrode for the $As^{III}$ analysis [53-54]. BiFE is suitable to be used as a working electrode in CSV because it provides a wide negative potential window similar to mercury electrode, while it is negligibly toxic comparing to mercury. It was found that the absence of $As^{III}$ peak current was observed. Therefore, this approach has been given up and may be studied in the further development.
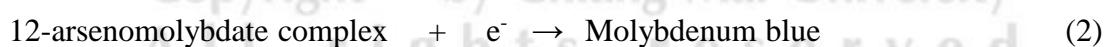
**3.2 Optimization cyclic voltammetric system for determination of arsenate**

This work aims to develop CV method for determination of $As^V$ using GCE as a working electrode. The parameters in CV for $As^V$ analysis as shown in Table 3.4 were employed.

Table 3.4 Conditions of CV for determination of arsenate

| Parameter | Conditions |
|---|---|
| Electrode: | |
| Working electrode | Glassy carbon electrode |
| Reference electrode | Ag/AgCl |
| Auxiliary electrode | Pt |
| Stirring rate | 2,000 rpm |
| Voltage step | 4 mV |
| Sweep rate | 100 mV s$^{-1}$ |
| Scanning potential: | |
| Initial potential | 100 mV |
| End potential | 550 mV |

The CV method is based on the molybdenum blue reactions. The reactions as follows [55-56]:

$$As^V \quad + \quad \text{Acidic molybdate} \quad \rightarrow \quad \text{12-arsenomolybdate complex} \qquad (1)$$

$$\text{12-arsenomolybdate complex} \quad + \quad e^- \quad \rightarrow \quad \text{Molybdenum blue} \qquad (2)$$

$$\text{or for step (2)} \quad Mo^{VI} \quad + \quad e^- \quad \rightarrow \quad Mo^V \qquad (3)$$

This reaction has been proposed based on the phosphate's reaction with molybdate to form molybdenum blue in acidic medium, usually detected by spectrophotometry. Alternatively, the cyclic voltammetric method for $As^V$ determination using the same reaction (reaction (1)) would be possible. The procedure in CV for $As^V$ analysis is described in section 2.5.

35

### 3.2.1 Concentration of molybdate

The effect of molybdate concentration was investigated by considering calibration graph of 2 to 10 mg $L^{-1}$ $As^V$ in 2.5% (v/v) $H_2SO_4$. A plot of the slope of the calibration graphs versus concentration of molybdate is shown in Figure 3.11. It was found that sensitivity increased when concentration of molybdate is increased. At the concentration of molybdate higher than 0.5% (w/v) sensitivity slightly decreased may be due to precipitation of the complex. Thus, the concentration of molybdate at 0.5% (w/v) was selected for the next experiment.
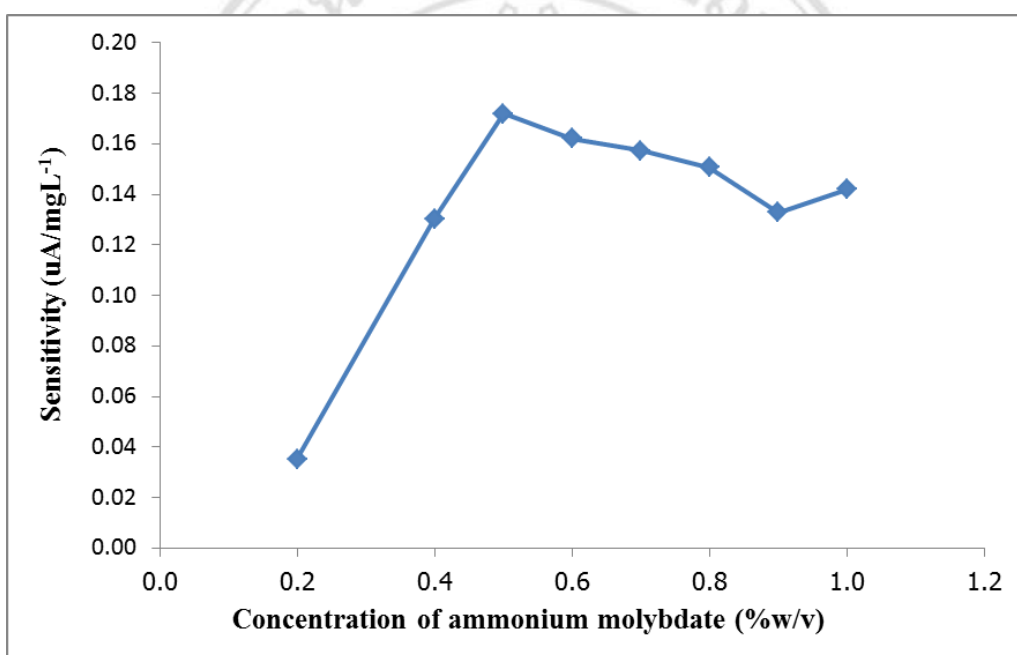


Figure 3.11 Effect of molybdate concentration in 2.5 % (v/v) $H_2SO_4$

**3.2.2 Concentration of sulfuric acid**

The effect of sulfuric acid concentration was investigated by considering calibration graph of 2 to 10 mg $L^{-1}$ $As^V$ in 0.5% (w/v) molybdate. A plot of the slope of the calibration graphs versus concentration of sulfuric acid is shown in Figure 3.12. Concentration of sulfuric acid at 2.0% (v/v) was selected for further study because it provides the highest sensitivity.
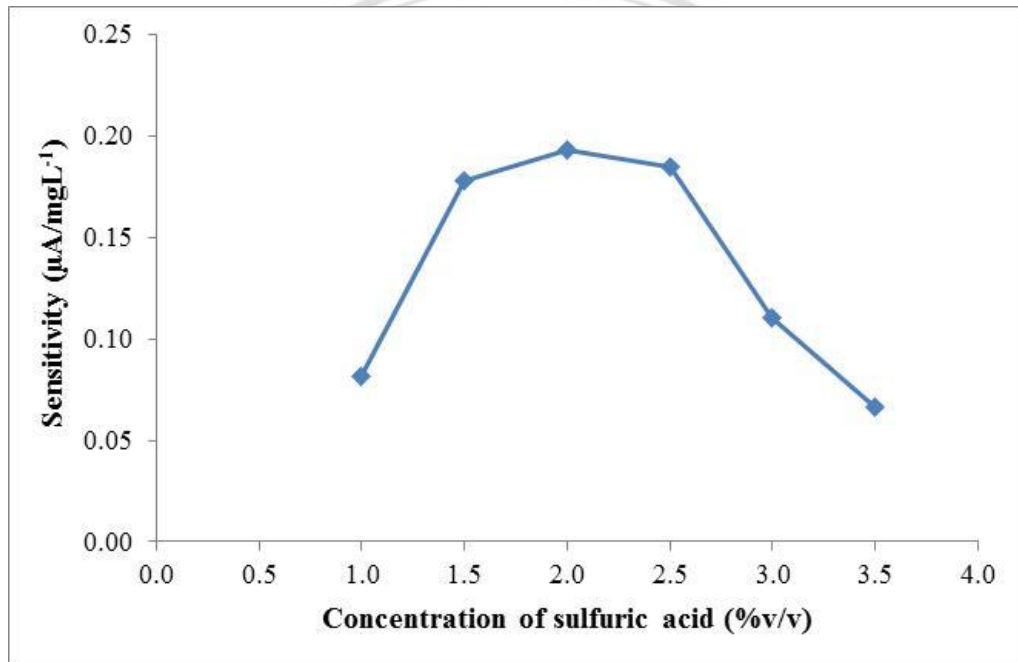


Figure 3.12 Effect of sulfuric acid concentration in 0.5 % (w/v) molybdate

### 3.2.3 Concentration of potassium antimonyl tartrate

A potassium antimonyl tartrate as a catalyst has been used for spectrophotometric determination of phosphorus [57]. The effect of potassium antimonyl tartrate concentration was investigated by considering calibration graph of 10 to 100 µg $L^{-1}$ As$^V$ in acidic molybdate. Slope, equation and $r^2$ of the calibration graphs are shown in Table 3.5. A plot of the slope of the calibration graph versus concentration of potassium antimonyl tartrate is shown in Figure 3.13. It was found that without potassium antimonyl tartrate the lowest sensitivity was obtained. The concentration of potassium antimonyl tartrate at 0.0002% (w/v) was chosen because it provides higher peak current than other concentrations (Table 3.5).

Table 3.5 Calibration graph data using different potassium antimonyl tartrate concentration

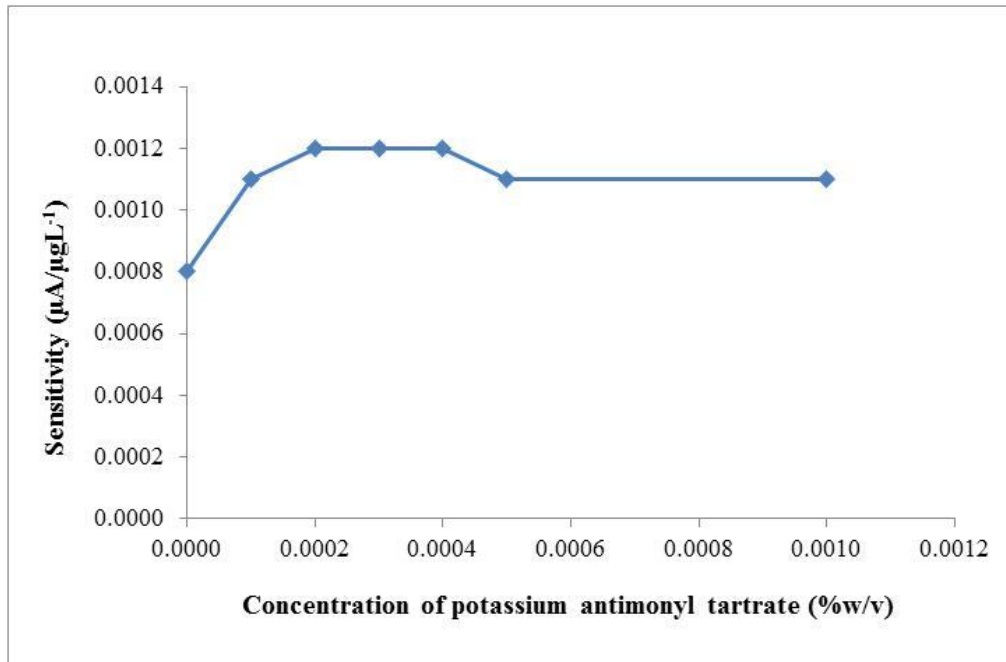| Concentration of potassium antimonyl tartrate (%w/v) | Slope (µA/µgL$^{-1}$) | Equation | $R^2$ |
|---|---|---|---|
| 0 | 0.0008 | y = 0.0008x + 0.2823 | 0.9977 |
| 0.0001 | 0.0011 | y = 0.0011x + 0.334 | 0.9920 |
| 0.0002 | 0.0012 | y = 0.0012x + 0.3443 | 0.9985 |
| 0.0003 | 0.0012 | y = 0.0012x + 0.327 | 0.9996 |
| 0.0004 | 0.0012 | y = 0.0012x + 0.3215 | 0.9984 |
| 0.0005 | 0.0011 | y = 0.0011x + 0.3106 | 0.9957 |
| 0.0010 | 0.0011 | y = 0.0011x + 0.2768 | 0.9940 |

Figure 3.13 Effect of potassium antimonyl tartrate concentration in acidic molybdate
(0.5% (w/v) molybdate in 2.0% (v/v) $H_2SO_4$)

### 3.2.4 Effect of scan rate

From the Randles-Sevcik equation as described in section 1.3.2. The peak current ($i_p$) is directly proportional to the square root of the scan rate ($\sqrt{v}$).

$$i_p = \sqrt{v}$$

The effect of the scan rate on the peak current was studied in the range of 50 and 150 mV s$^{-1}$ at 5 mg L$^{-1}$ As$^V$. A linear relationship was observed between the oxidation peak current versus the square root of scan rate (Figure 3.14) indicate that the electrode process is diffusion controlled. The scan rate at 100 mV s$^{-1}$ was selected for further study.
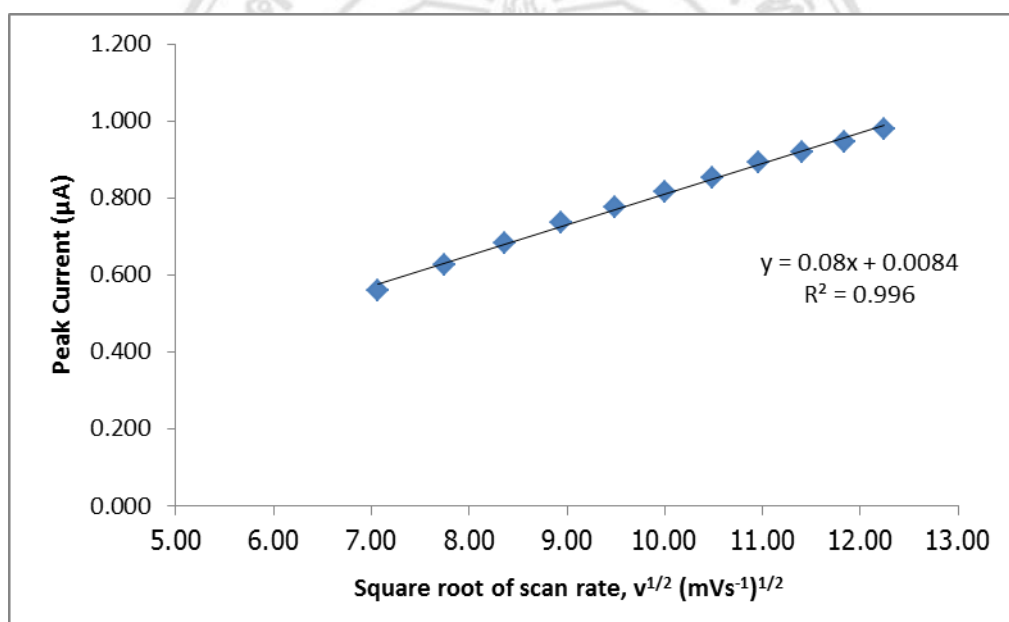


Figure 3.14 Effect of scan rate on the peak current of 5 mg L$^{-1}$ As$^V$ (0.5% (w/v) molybdate in 2.0% (v/v) H$_2$SO$_4$)

### 3.2.5 Effect of working electrode

A glassy carbon disc (3 mm diameter) and platinum disc (3 mm diameter) working electrode were studied. The effect of working electrode was investigated by considering calibration graphs for each linear range of $As^V$ determination. Slope, regression equation and $r^2$ of the calibration graphs are shown in Table 3.6. It was found that the GCE provide higher sensitivity than Pt electrode. Thus, the GCE was chosen for further experiments.

Table 3.6 Calibration graph data for each linear range of $As^V$ determination using different working electrodes

| Range of $As^V$ concentration (mgL$^{-1}$) | Electrode | Calibration graph data | | |
|---|---|---|---|---|
| | | Slope ($\mu$A/mgL$^{-1}$) | Equation | $R^2$ |
| 1-10 | GCE | 0.1832 | y = 0.1832x + 1.196 | 0.9990 |
| | Pt | 0.1531 | y = 0.1531x - 0.0276 | 0.9992 |
| 0.1-1 | GCE | 0.5613 | y = 0.5613x + 0.5158 | 0.9962 |
| | Pt | 0.1409 | y = 0.1409x + 0.0459 | 0.9921 |
| 0.01-0.1 (10-100 $\mu$gL$^{-1}$) | GCE | 0.6822 | y = 0.6822x + 0.3181 | 0.9987 |
| | Pt | 0.1521 | y = 0.1521x + 0.0126 | 0.9876 |

### 3.2.6 Analytical characteristics of the system

#### 3.2.6.1 Calibration curves and limit of detection

Using the selected condition, the calibration graph of $As^V$ in different concentration ranges 10-100 μg $L^{-1}$, 0.05-0.4 mg $L^{-1}$ and 1-10 mg $L^{-1}$ were obtained, as the voltammograms of $As^V$ shown in Figure 3.15. The linear calibration graph of 10-100 μg $L^{-1}$ $As^V$, 0.05-0.4 mg $L^{-1}$ $As^V$ and 1-10 mg $L^{-1}$ $As^V$ were (y = 0.0006x + 0.0275, $r^2$ = 0.9977), (y = 0.6102x + 0.0255 ,$r^2$ = 0.9985) and (y = 0.1127x + 0.2636, $r^2$ = 0.996), respectively (Figure 3.16). The LOD was calculated from the lowest linear range of the calibration graph [58] and found to be 6.94 ng $L^{-1}$. The results are given in Appendix C.
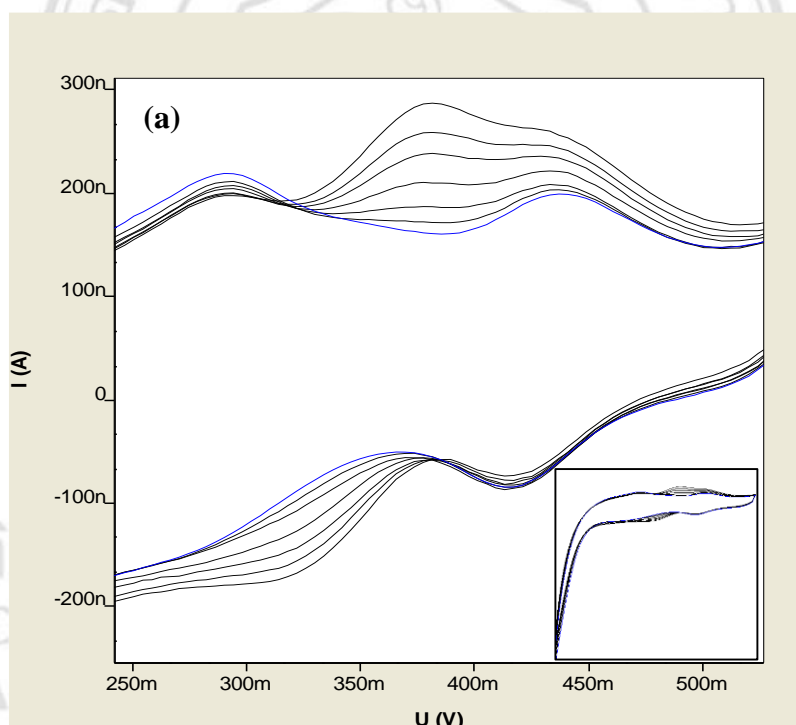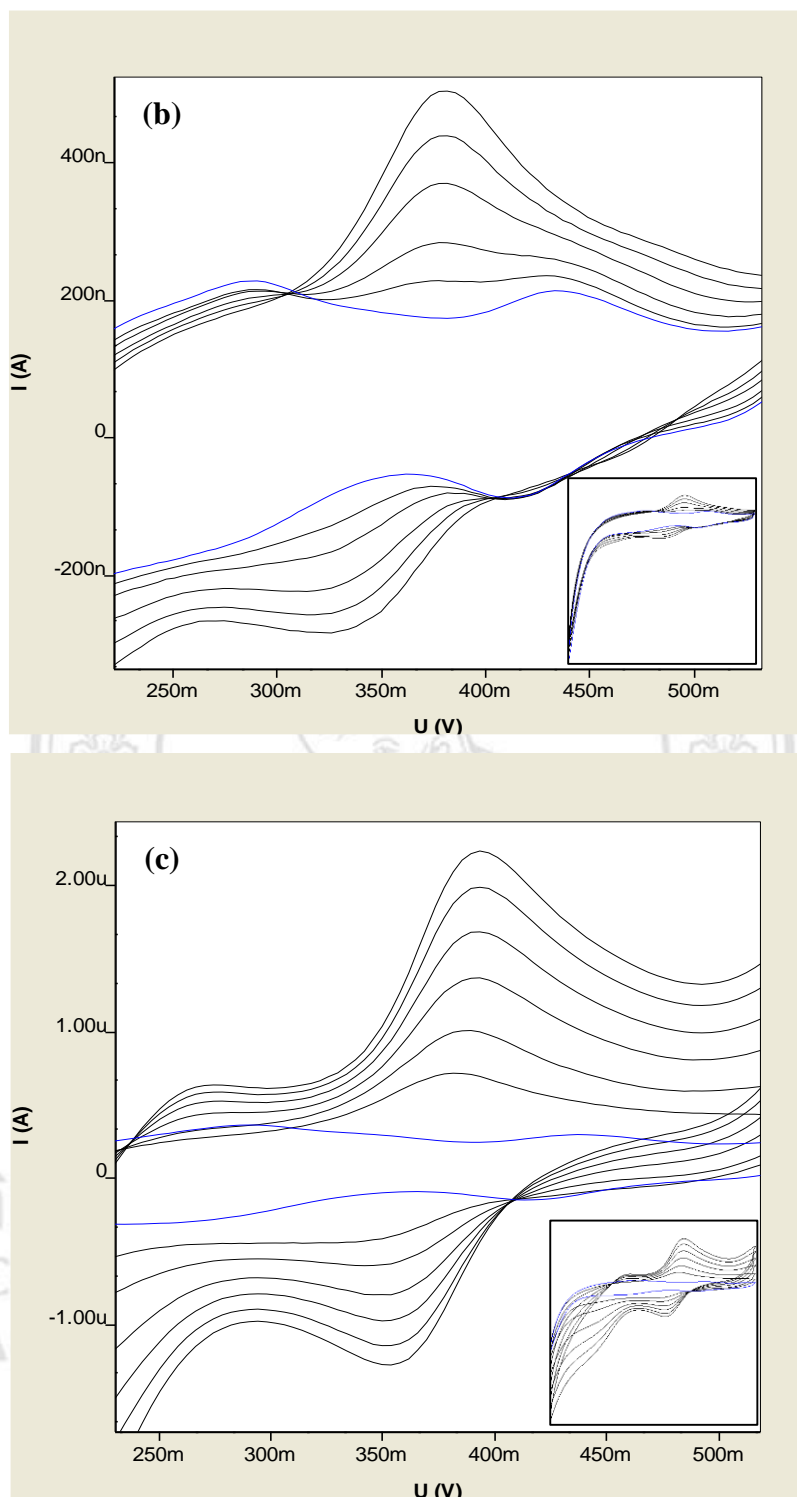
Figure 3.15 Voltammograms of $As^V$ in various concentration ranges: (a) 10-100 μg $L^{-1}$, (b) 0.05-0.4 mg $L^{-1}$ and (c) 1-10 mg $L^{-1}$
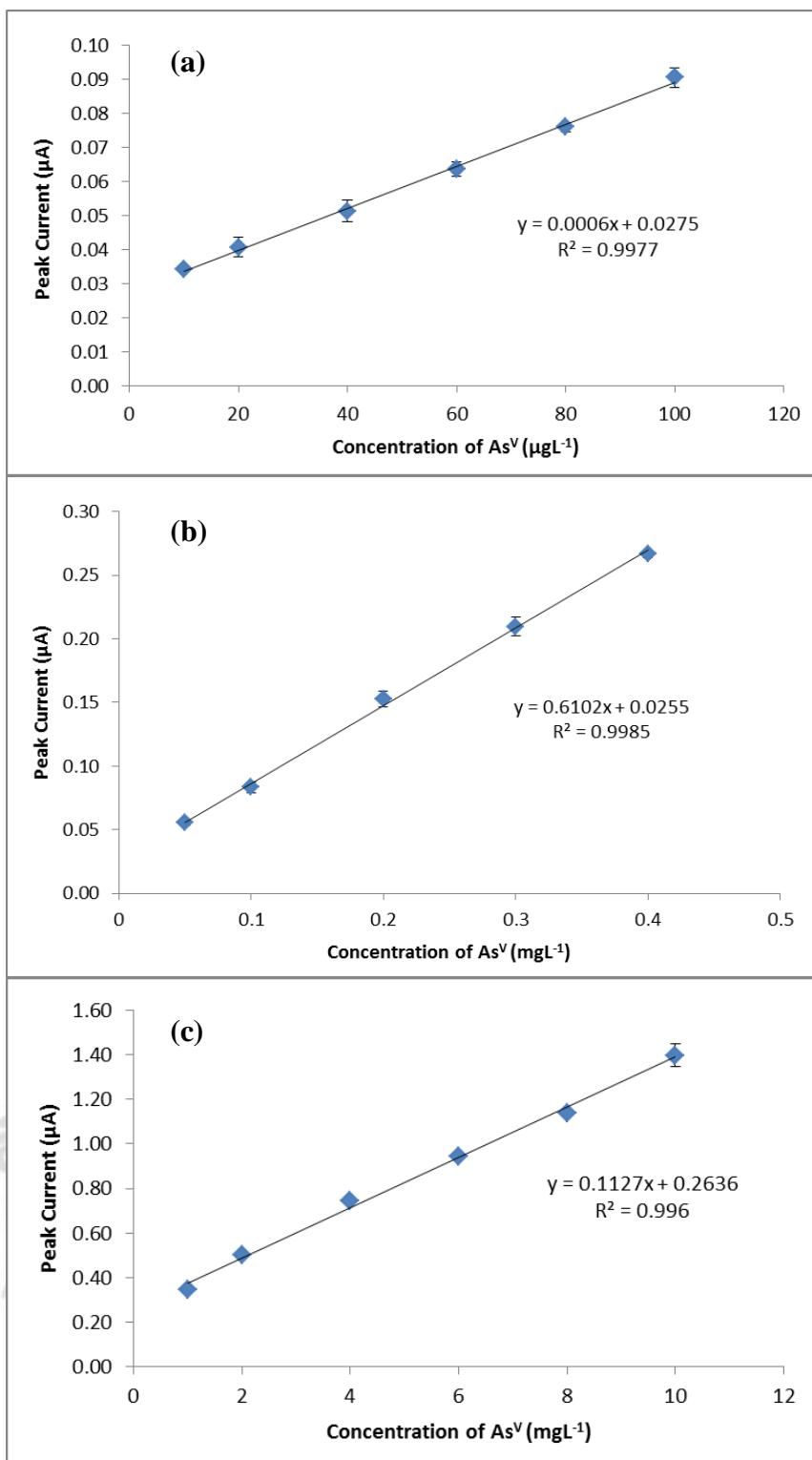
Figure 3.16 Calibration graphs of As$^V$ in various concentration ranges:
(a) 10-100 µg L$^{-1}$, (b) 0.05-0.4 mg L$^{-1}$ and (c) 1-10 mg L$^{-1}$

### 3.2.6.2 Precision

The precision of the system was verified by 11 replicated determination of standard solution of $As^V$ at 50 µg $L^{-1}$ (ppb) and 0.2 mg $L^{-1}$ (ppm). The percentage of relative standard deviation (%RSD) values was used for evaluating the precision and can be calculated from the equation (2.4). The relative standard deviations of 11 replicate were 3.72% for 50 µg $L^{-1}$ and 2.71% for 0.2 mg $L^{-1}$ $As^V$. The results are given in Table 3.7, indicated a good reproducibility of the method.

Table 3.7 The precision of standard $As^V$ determination by cyclic voltammetric system

| Number | Peak current (µA) | |
| --- | --- | --- |
| | 50 µg $L^{-1}$ | 0.2 mg $L^{-1}$ |
| 1 | 0.051 | 0.164 |
| 2 | 0.053 | 0.169 |
| 3 | 0.056 | 0.171 |
| 4 | 0.054 | 0.176 |
| 5 | 0.056 | 0.174 |
| 6 | 0.058 | 0.175 |
| 7 | 0.058 | 0.171 |
| 8 | 0.055 | 0.177 |
| 9 | 0.055 | 0.178 |
| 10 | 0.054 | 0.179 |
| 11 | 0.055 | 0.179 |
| Mean | 0.055 | 0.174 |
| SD | 0.002 | 0.005 |
| %RSD | 3.72 | 2.71 |

45

### 3.2.7 Application to real sample

The proposed method was applied to determine $As^V$ in real water samples. The results obtained from the standard addition method for 9 water samples are shown in Table 3.8. The method has percentage recoveries for the determination of $As^V$ in the range of 85.6 - 95.4. The results are given in Appendix D. Samples were also analyzed by anodic stripping voltammetric method. The ASV method only measures $As^{III}$, the reduction of $As^V$ to $As^{III}$ by L-cysteine is essential prior to ASV determination. Concentration of $As^V$ was calculated by subtracting of total As concentration (after reduction) with $As^{III}$ concentration (before reduction). The results obtained from both the methods are presented in Table 3.9.

Table 3.8 Determination of $As^V$ in water samples by cyclic voltammetry

| Sample | Concentration of $As^V$ (mg $L^{-1}$) [a] | % Recovery |
|--------|------------------------|------------|
| 1 | 2.7±0.3 | 93.7 |
| 2 | 2.3±1.3 | 95.4 |
| 3 | 2.4±0.0 | 94.4 |
| 4 | 2.8±0.6 | 93.5 |
| 5 | 4.0±0.7 | 89.7 |
| 6 | 2.7±0.7 | 92.9 |
| 7 | 4.1±0.9 | 87.4 |
| 8 | 5.0±0.1 | 85.6 |
| 9 | 3.6±0.3 | 88.7 |

[a] Mean of duplicate results

Table 3.9 Comparative determination of $As^V$ in water sample by cyclic voltammetry
and anodic stripping voltammetry

| Sample | Concentration of $As^V$ (mg $L^{-1}$) [a] | | % Difference |
| | CV | ASV | |
|---|---|---|---|
| 1 | 2.7±0.3 | 3.2 ±0.1 | -15.63 |
| 2 | 2.3±1.3 | 4.5 ±0.6 | -48.89 |
| 3 | 2.4±0.0 | 3.7 ±0.2 | -35.14 |
| 4 | 2.8±0.6 | 3.2 ±0.3 | -12.50 |
| 5 | 4.0±0.7 | 4.9 ±0.6 | -18.37 |
| 6 | 2.7±0.7 | 4.2 ±0.1 | -35.71 |
| 7 | 4.1±0.9 | 7.1 ±0.1 | -42.25 |
| 8 | 5.0±0.1 | 3.0 ±0.1 | 66.67 |
| 9 | 3.6±0.3 | 3.6 ±0.2 | 0 |

[a] Mean of duplicate results

From Table 3.9 it was found that the results obtained by ASV method had a more
positive bias than those obtained by proposed CV method. This might be because of the
interference in water samples.